horticulturae

MDPI

Article

Identification of *Botrytis cinerea* as a Walnut Fruit Rot Pathogen, and Its Biocontrol by *Trichoderma*

Andrea Zabiák [1,†], András Csótó [2,†], Károly Pál [1], Erzsébet Fekete [3], Levente Karaffa [3] and Erzsébet Sándor [2,*]

[1] Institute of Food Science, Faculty of Agricultural and Food Science and Environmental Management, University of Debrecen, Böszörményi út 138., H-4032 Debrecen, Hungary; zabiak.andrea@agr.unideb.hu (A.Z.); pal.karoly@agr.unideb.hu (K.P.)
[2] Institute of Plant Protection, Faculty of Agricultural and Food Science and Environmental Management, University of Debrecen, Böszörményi út 138., H-4032 Debrecen, Hungary; csoto.andras@agr.unideb.hu
[3] Department of Biochemical Engineering, Faculty of Science and Technology, University of Debrecen, Egyetem tér 1., H-4032 Debrecen, Hungary; kicsizsoka@yahoo.com (E.F.); karaffa.levente@science.unideb.hu (L.K.)
* Correspondence: karaffa@agr.unideb.hu
† These authors contributed equally to this work.

Abstract

Walnut (*Juglans regia* L.) fruit rot significantly impacts yield and quality, yet the pathogens responsible for it remain insufficiently characterized. In this study, we identified several fungi associated with the disease and characterized their morphology and physiology. Pathogenicity tests at two developmental stages of the walnut fruit were performed for the newly described pathogen. Among the *Botrytis*, *Alternaria*, and *Penicillium* species, *Botrytis cinerea sensu lato* stands out as a newly identified pathogen of the cultivated walnut. Growth assessments revealed variability in *B. cinerea* strains, with consistent patterns found across different temperatures. Pathogenicity of the isolated *B. cinerea* strains differed: one strain caused husk necrosis, three strains caused kernel necrosis in younger fruits, while two strains induced kernel necrosis in the later developmental stages. Additionally, we evaluated the biocontrol potential of *Trichoderma* strains against *B. cinerea* and demonstrated their efficiency in suppressing each isolated *B. cinerea* strain (76–100% inhibition), highlighting their potential in sustainable disease management in walnut production.

Keywords: *Juglans regia* L.; biocontrol; green walnut pathogen fungi; ONFIT test

Academic Editors: Piao Yang, Wei Wei and Ling Lu

Received: 16 May 2025
Revised: 18 June 2025
Accepted: 20 June 2025
Published: 22 June 2025

Citation: Zabiák, A.; Csótó, A.; Pál, K.; Fekete, E.; Karaffa, L.; Sándor, E. Identification of *Botrytis cinerea* as a Walnut Fruit Rot Pathogen, and Its Biocontrol by *Trichoderma*. *Horticulturae* **2025**, *11*, 725. https://doi.org/10.3390/horticulturae11070725

1. Introduction

Walnut cultivation plays a significant role in global agricultural production, particularly in major walnut-producing countries such as China and the United States [1]. However, the increasing prevalence of pathogens and pests threatens the global cultivation of 3.989 million tons of shelled walnuts [2]. These biotic stresses lead to yield losses and reduced fruit quality, manifested through leaf spots, root rot, and fruit malformations–posing significant economic risks to growers [3–7].

In Hungary, walnut (*Juglans regia* L.) is the third most widely cultivated fruit, accounting for 5.1% of the country's total fruit production. Hungary produces approximately 5500 tons of walnuts annually, cultivated across 7900 hectares [2]. Walnuts are rich in essential fatty acids, proteins, vitamins, and minerals. This nutrient-dense profile highlights their significance in the human diet [8].

Young walnuts, especially before shell hardening, are highly susceptible to pathogen attacks, with the green husk remaining vulnerable even afterward [6]. *Xanthomonas arboricola* pv. *juglandis*, the causal agent of walnut blight, significantly reduces yields in high-rainfall regions [9]. A fungal survey of immature walnuts identified numerous pathogenic Ascomycota species [10]. *Colletotrichum* species, responsible for anthracnose, have been reported in both Chinese and Hungarian walnut orchards [11,12]. Additionally, *Botryosphaeria dothidea*, *Diaporthe eres*, and *Diplodia seriata* cause necrotic lesions on green husks, often leading to extensive tissue decay [6,10,13].

Botrytis cinerea, a polyphagous fungal pathogen, infects various tree nuts, including pecans, chestnuts, and hazelnuts, causing necrotic lesions on nuts and leaves [14–16]. Initial symptoms include small, water-soaked leaf spots that expand into brown or gray lesions with a yellow halo. Severe infections result in leaf wilting, cankers, dieback, and fruit rot, with affected nuts covered in gray mold [17]. Although it was reported to be present on stored walnuts [18,19] its pathogenicity has never been proved.

Environmental factors strongly influence *B. cinerea* infection. Optimal growth occurs at 18–24 °C, while temperatures above 32 °C inhibit its development. High relative humidity ($\geq$93%) and prolonged leaf wetness facilitate spore germination, with dense canopies creating microclimates conducive to infection [20].

Fungicide resistance presents a major challenge in *B. cinerea* management, as the extensive use of synthetic fungicides has led to resistant strains, reducing treatment efficacy [21]. Sustainable alternatives, such as biological control agents, are gaining importance. *Trichoderma* spp. offer effective biocontrol through mycoparasitism, competition, and systemic resistance induction toward several plant pathogen fungi [22–24].

The objective of this study was to identify the pathogen composition in symptomatic green walnut fruits, and identify the primary pathogen responsible for early fruit damage. We confirmed the pathogenicity of the newly described *B. cinerea*, and propose a sustainable control strategy. Additionally, this research offers insights into the environmental and phenological requirements of the main pathogen, providing practical guidance for the development of effective plant protection technologies.

2. Materials and Methods

2.1. Origin and Description of Plant Samples

A total of 52 green walnuts ('Milotai bőtermő' cultivar) exhibiting symptoms of brown lesions and spots on the husk were collected from Nagyszekeres, northeastern Hungary, in early summer at 2023. In the orchard, fruits with dark lesions were collected from trees both directly and after shaking. Only freshly fallen fruits were collected. Fungicide treatments containing copper, sulfur, and tebuconazole were applied in the orchard during the pre-sampling period (Table 1).

Table 1. Fungicide treatments in the sampled plantation.

Date	Active Ingredient	Dose (g/ha)
20 March 2023	CuOCl + S	1595 + 4000
28 April 2023	tebuconazole	180
12 May 2023	tebuconazole	250
1 June 2023	CuOCl + S	1595 + 4000

2.2. ONFIT Assay

To detect causal pathogens, the Overnight Freezing-Incubation Technique (ONFIT) method [7,25,26] was used. Samples were surface-disinfected using the method described by Kovács et al. (2014) [27] to eliminate surface contaminants. A 10% chlorogen-

sesquihydrate (Neomagnol; Parma Produkt Ltd., Budapest, Hungary) and 0.1% Tween20 (Merck KGaA, Darmstadt, Germany) solution was employed for one-minute disinfection of fruit surfaces, followed by two washes in sterile distilled water. Following surface disinfection, walnuts were incubated at −16 °C for 15 h to disrupt fungistatic compounds within the fruit tissues [28]. Subsequently, walnuts were transferred to sterile containers and incubated at 25 °C and 95% relative humidity for 14 days in the dark. The emergence of mycelia on the husk surface indicated fungal infections. To isolate individual fungal strains, hyphal tips were carefully extracted from fungal colonies growing on agar plates. Each tip was then transferred to a fresh potato dextrose agar (PDA, Scharlau, Barcelona, Spain) medium. This process, was repeated multiple times to ensure the purity of the fungal cultures [29].

2.3. Morphological and Molecular Characterization of Fungal Isolates

For preliminary genus-level identification, macroscopic characteristics such as colony color and texture were examined on PDA. Microscopic features were determined using a Nikon Eclipse Ni light microscope (Tokyo, Japan).

Genomic DNA was extracted from the cultures using a NucleoSpin Plant II Kit (Macherey-Nagel, Düren, Germany) following the manufacturer's protocol. Isolates were cultured on PDA medium for seven days. Subsequently, mycelia were transferred to 2-mL BashingBead tubes (Zymo Research Corp., Irvine, CA, USA) containing 0.7 mL of 2-mm ceramic beads and 500 µL lysis buffer.

PCR reactions were performed to amplify the ITS region using ITS1 (5′-TCCGTAGGTGAACCTGCGG-3′) and ITS4 (5′-TCCTCCGCTTATTGATATGC-3′) (IDT, Leuven, Belgium) primers [30] and a Bio-Rad T100 thermocycler (Bio-Rad Laboratories, Inc., Hercules, CA, USA). The final reaction volume was 25 µL, containing 12.5 µL DreamTaq Green Master Mix (Thermo Scientific, Vilnius, Lithuania), 0.5 µL of each primer (10 pmol/µL), 10.5 µL of nuclease-free water, and 1 µL of DNA template (10 ng/µL).

Amplification began with an initial denaturation step at 95 °C for 3 min, followed by 35 cycles of 30 s at 95 °C, 45 s at 56 °C, and 60 s at 72 °C. A final extension step was performed at 72 °C for 5 min. PCR product amplification was verified by electrophoresis on a 1% agarose gel (Bioline Memphis, TN, USA) stained with 4 µL of EcoSafe (Pacific Image Electronics, New Taipei, Taiwan) and run at 100 V for 60 min using a Bio-Rad electrophoresis system. A 5-µL FastRuler Low Range DNA ladder (Thermo Scientific, Vilnius, Lithuania) was loaded for size determination.

PCR products were purified using a NucleoSpin Gel and PCR Clean Up Kit (Macherey-Nagel). Purified PCR products were sent to Microsynth GmbH (Vienna, Austria) for Sanger sequencing using ITS1 as primer. The obtained sequences were analyzed using the BLASTN algorithm and compared to type strains in the GenBank database of NCBI. Phylogenetic analysis was performed using the MEGA 7.0 software [31]. Maximum likelihood was employed to infer phylogenetic trees, with the Kimura 2-parameter model of nucleotide substitution [32]. The robustness of the resulting tree topology was evaluated using a heuristic search algorithm based on nearest-neighbor interchange. Branch support values were determined by performing 1000 bootstrap replicates to assess the statistical confidence of the internal nodes.

2.4. Determination of Optimal Growth Temperatures for Botrytis cinerea Isolates

To determine the optimal growth temperature, four isolates of *Botrytis cinerea* (J5011/1, J5013/1, J5017, J5021) were cultured on potato dextrose agar (PDA) at 20 °C. For each isolate, five replicated agar plates were used. After seven days of incubation, 4-mm-diameter mycelial plugs were removed from the actively growing colony margins and transferred to

fresh PDA plates in five replicates. These plates were then incubated at 15, 20, 25, and 30 °C under dark conditions. Isolates whose growth was inhibited at elevated temperatures were subsequently incubated at 20 °C to investigate the impact of temperature on their viability. Colony diameters were measured daily from the third day until the seventh day.

2.5. Pathogenicity Test

To investigate the pathogenicity of pathogen isolates, artificial inoculations were conducted on green walnuts. To assess the impact of developmental stage of the walnut fruits on disease severity, the test was repeated at two growth stages, BBCH 75 and 79 [33]. The previously studied four *Botrytis cinerea* (J5011/1, J5013/1, J5017, J5021) isolates were used as pathogens based their different morphological characters. The experiment was conducted with five replicates, and five control walnuts were inoculated with sterile PDA disks.

Prior to inoculation, the walnut surface was sterilized with 70% ethanol. A sterile toothpick was used to create a wound, onto which a 4-mm agar disk containing actively growing mycelium of the pathogen was inserted. The wound was sealed with sealing film (Parafilm M, Bemis, Sheboygan Falls, WI, USA), to prevent desiccation. Inoculated walnuts were incubated in a growth chamber at 25 °C for three weeks under high humidity conditions in the dark.

The severity of husk necrosis was assessed using a scale described previously that ranges from 0, indicating the complete absence of symptoms, to 5, which signifies complete rot [6]. Kernel necrosis was quantified as a percentage of the total kernel area. The virulence of the pathogen was also characterized based on disease severity index [34].

2.6. Dual Culture Test of Botrytis cinerea and Trichoderma spp.

Dual culture assays were conducted to assess the antagonistic potential of TR04 *Trichoderma afroharzianum* and TR05 *Trichoderma simmonsii* against the four *Botrytis cinerea* isolates (J5011/1, J5013/1, J5017, J5021). Mycelial discs were excised from the actively growing margin of 7-day-old cultures and placed three cm from the center of a PDA plate, in five replicates. Plates containing only the pathogenic fungus served as a control. Colony diameters were measured on days 3, 8, and 10, and growth inhibition was calculated, as follows:

$$I\% = [(dc - dt)/dc] \times 100,$$

I%: inhibition percentage; where dc: diameter of mycelial growth on PDA without biocontrol agent; dt: diameter of mycelial growth in confrontation with *Trichoderma* sp.

2.7. Statistical Analysis

To compare the means of the assessed data non-parametric tests were used since the assumptions of parametric tests (normal distribution and homoscedasticity) were not fulfilled. If the Kruskall-Wallis test was significant ($p < 0.05$), pairwise group comparisons using the Mann-Whitney U test ($p < 0.05$) were performed, and the resulting significant differences were visualized using a compact letter display (CLD). Data processing was performed in MS Excel 365, statistical analysis was conducted in SPSS 29.

3. Results

3.1. Assessment of Symptoms of Immature Walnuts

Symptoms with different severity were detected on the immature walnut fruits, which were indicative of a fungal infection (Figure 1). In the orchard, fruits with dark lesions were collected from trees both directly and after shaking, ensuring only freshly fallen ones

were gathered. Symptomatic fruits had broad severity scales, ranging from mild to severe decaying symptoms.

(**a**) (**b**) (**c**)

Figure 1. The broad spectrum of symptoms on walnuts; (**a**) small brown lesion, as an initial symptom; (**b**) extended necrotic lesion; (**c**) advanced stage of the disease.

Small, circular dark brown lesions appeared on the husk, indicating initial symptoms (Figure 1a). These lesions expanded, coalesced, and developed into larger, irregular, sunken areas with progressed disease. The necrotic tissue was often surrounded by a distinct halo, indicating a more advanced stage of decay (Figure 1b). In severe cases, the entire surface of the husk was covered by these lesions, leading to premature abscission (Figure 1c). Husk cracking was another common symptom, often associated with the underlying lesions.

3.2. ONFIT Assay Results

Using ONFIT method, a wide range of fungal genera were detected on green walnuts (Table 2).

Table 2. Isolated genera from symptomatic green walnuts following ONFIT.

Genus	Number of Infected Fruits
Aspergillus	19
Botryosphaeria	2
Botrytis	37
Fusarium	2
Penicillium	19
Diaporthe	1

3.3. Morphological and Molecular Characterization of Casual Pathogens

The results indicated that *Botrytis*, *Aspergillus*, and *Penicillium* species were the most prevalent fungal genera, isolated from 37 (71.2%), 19 (36.5%), and 19 (36.5%) fruits, respectively (Figure 2). *Alternaria*, *Botryosphaeria*, *Diaporthe*, and *Fusarium* species were also identified, but their presence was considerably lower. *Botrytis* frequently co-occurred with both *Aspergillus* and *Penicillium*, in seven-seven cases (13.5%) coinfection was detected for each fungus. In three samples (5.8%), all the three fungal genera were simultaneously detected on the same walnut.

Botrytis sp. usually formed creamy orange colonies on the walnut husk surface, accompanied by the production of abundant, dense, white aerial mycelium (Figure 2a). Limited colony formation and sparse aerial mycelium was also detected in some cases, suggesting that *Botrytis* infection was developed only in an early stage (Figure 2b). *Penicillium* formed flat, green colonies on the sample surface, which were generally of limited extent (Figure 2c). *Aspergillus* species were identified by their characteristic small, black conidiophores, which were sometimes accompanied by abundant aerial mycelium (Figure 2c,d).

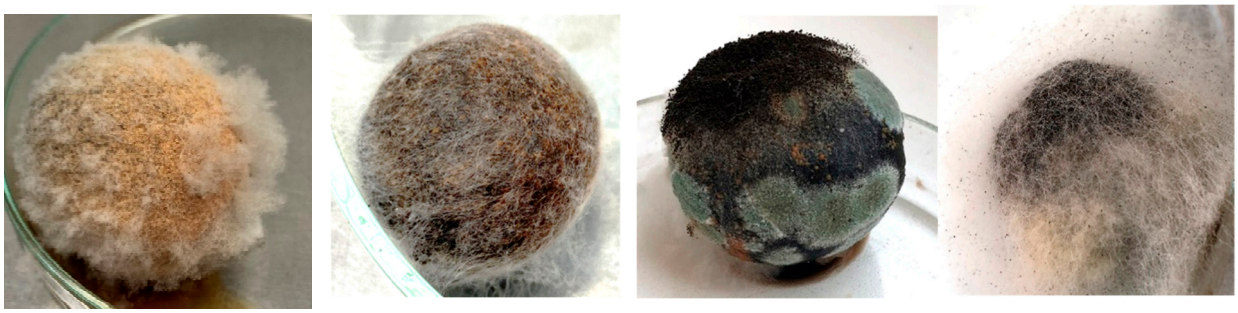

(**a**) (**b**) (**c**) (**d**)

Figure 2. Fungal mycelia developed after using the ONFIT process (**a**) *Botrytis* spp. with dense, white aerial mycelia; (**b**) *Botrytis* spp. with sparse aerial mycelia; (**c**) Green *Penicillium* colonies and black conidiophores of *Aspergillus* sp.; (**d**) abundant aerial mycelia of *Aspergillus* genus.

Botrytis isolates, when cultivated on PDA at 20 °C in the dark, exhibited a range of colony morphology characteristics (Figure 3). The majority of the isolates had limited aerial mycelium production; their growth was restricted to the agar surface. Only some of them produced fluffy or cottony structure. The color of the colonies varied between shades of white to gray and brown. The colonies were compact and homogeneous, without radial expansion. Mycelial nodulation was observed in some isolates as a precursor to sclerotia formation. Rapid sclerotia formation was observed in some isolates within 10 days.

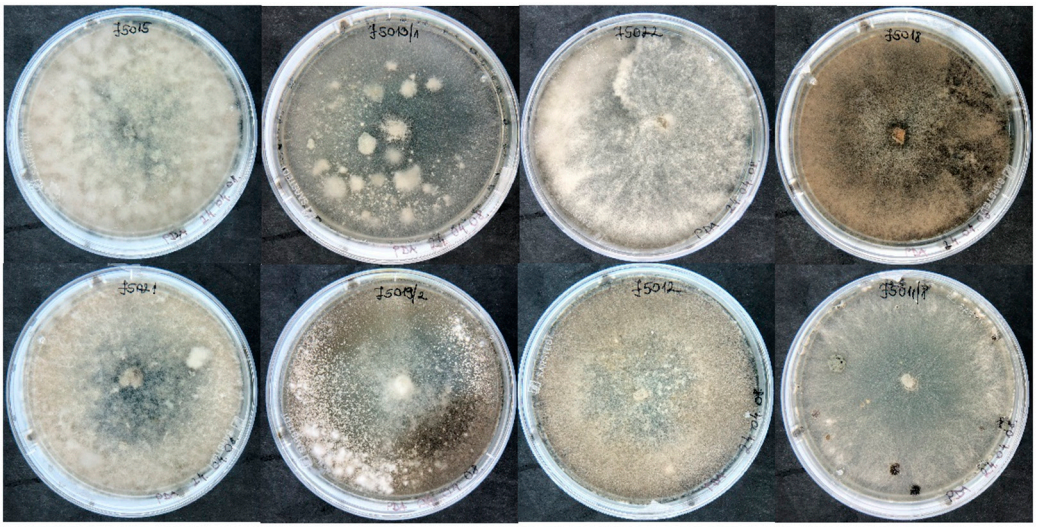

Figure 3. Colony morphology of various *Botrytis* isolates grown on PDA after 10 days.

Microscopic examination revealed presence of septate, hyaline hyphae and smooth, globose to subglobose conidia with a diameter ranging from 3 to 6 µm. Conidia were produced in small clusters on branched conidiophores (Figure 4a,b).

A total 8 out of 37 *B. cinerea* isolates with different colony morphological characters were chosen for sequence-based identification. Following PCR amplification of the rDNA region, containing ITS1 and ITS2 sequences, eight *B. cinerea* isolates were sequenced, and the resulting sequences were deposited into GenBank with accession numbers PV290581–PV290588 (Table 3).

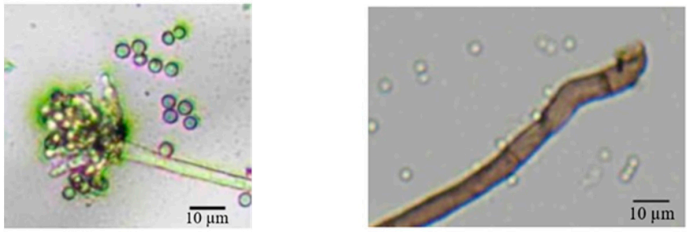

(**a**) (**b**)

Figure 4. (**a**) Typical spore-bearing structure and conidia of *Botrytis* sp.; (**b**) septate hyphae of a *Botrytis* sp. isolate.

Table 3. Accession numbers of the deposited ITS sequences of *Botrytis cinerea* isolates.

Isolate	Accession Number
J5008	PV290581
J509/2	PV290582
J5011/1	PV290583
J5013/3	PV290584
J5018	PV290585
J5021	PV290586
J5017	PV290587
J5012	PV290588

To confirm their identity, these sequences were subjected to BLASTN analysis against nucleotide databases and Molecular Phylogenetic analysis. The observed significant (100%) homology to known *B. cinerea* sequences conclusively identified all eight isolates as members of the *B. cinerea* species complex. The sequenced 384 bp identical with both *B. cinerea* type strains, B05.10 and T4, and another strain (GBC-32a, with sequence JN692382) as well as *B. pseudocinerea* isolate YC-7 (MF461632), *B. fabae* CBS109.57 (AJ716303) and *B. pelargonii* CCBS_497.50 (NR_159600). Phylogenetic analysis placed our strains within the *B. cinerea sensu lato* clade (Figure 5).

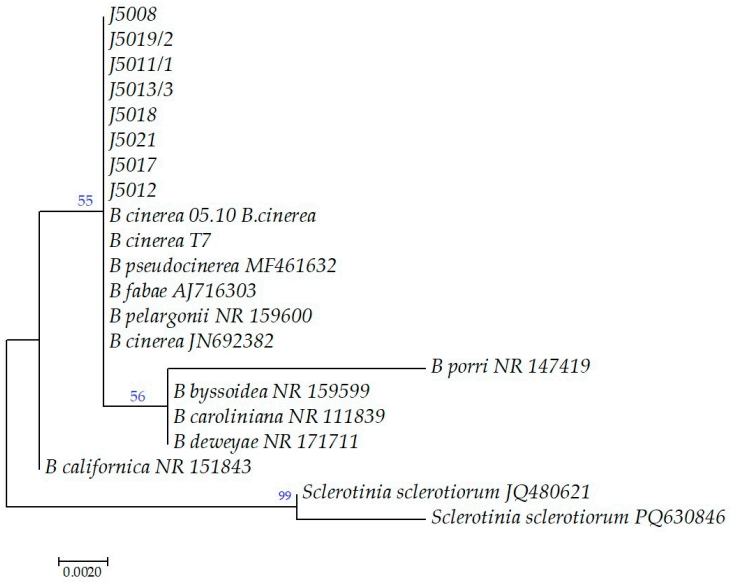

Figure 5. Maximum Likelihood tree of ITS sequences was constructed with MEGA7 [31]. Hungarian isolates are indicated with strain numbers only, while *Botrytis* species with strain numbers were collected from NCBI gene bank. The tree was rooted on *Sclerotinia sclerotiorum*. Branch support values (>50%) resulting from 1000 iterative bootstrap replicates are given above the nodes. The tree is drawn to scale, with branch lengths corresponding to the number of substitution per site, and the scale is shown under the dendrogram.

3.4. Temperature Growth Profiles of Botrytis cinerea Isolates

Given that all isolates possessed identical ITS sequences, we propose to test for variations in temperature growth among strains displaying diverse colony morphologies. This investigation seeks to elucidate the adaptive diversity of the pathogenic *B. cinerea* population in response to distinct environmental conditions within a given orchard.

Significant variations in growth rates were observed among strains and across temperature treatments (Figure 6). At 15 °C, clear differences in growth rates were observed among the four *Botrytis cinerea* isolates. Isolate J5013/3 exhibited the slowest growth, with colony diameters reaching only 57.4 mm after 7 days of incubation. J5017 and J5021 exhibited intermediate growth rates, and J5011/1 was the most vigorous at 15 °C, overgrown the entire medium (90 mm).

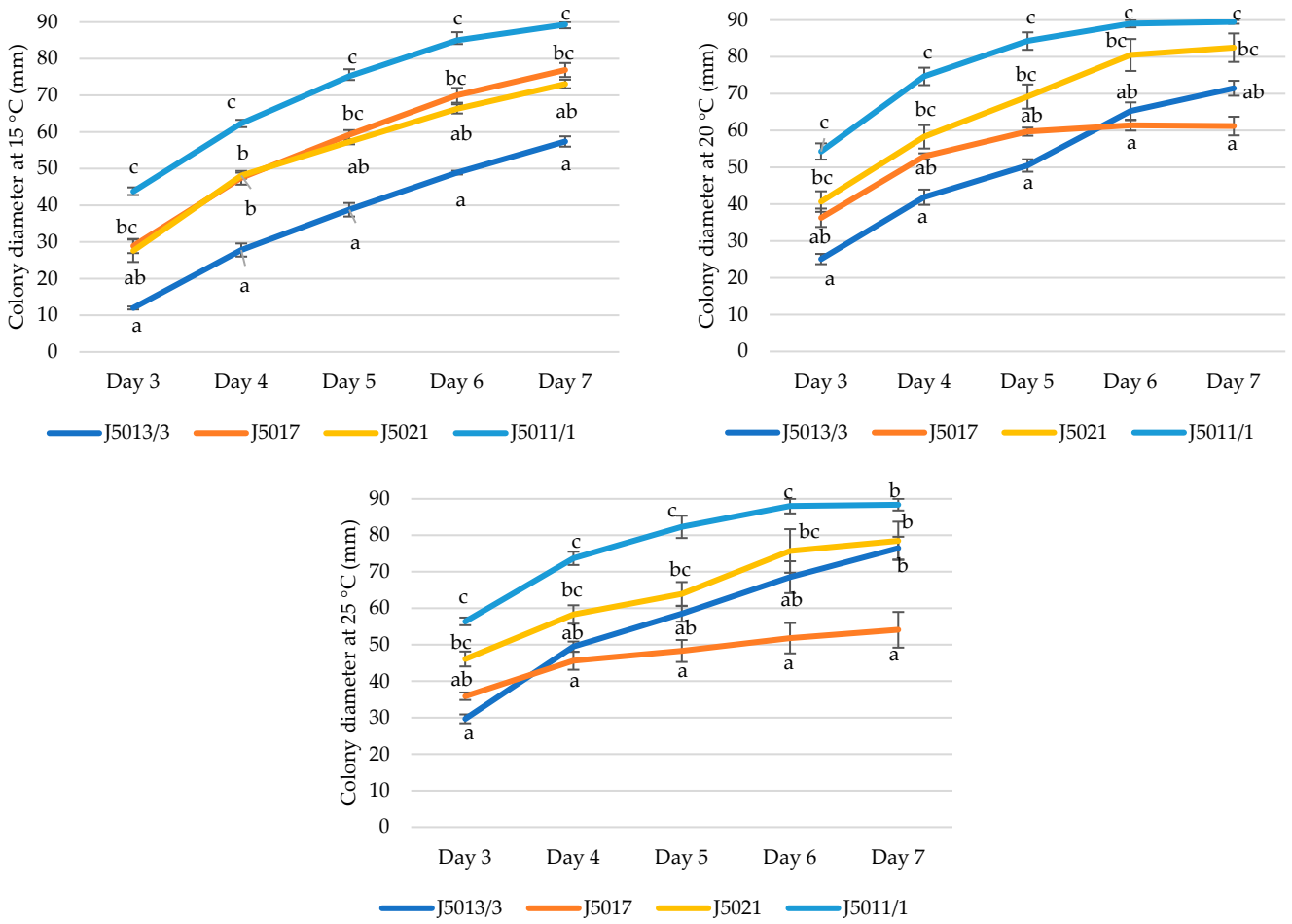

Figure 6. Effect of temperature on the growth of *Botrytis cinerea* isolates. CLD (lowercase letters) indicates statistical differences based on pairwise Mann-Whitney U tests ($p < 0.05$).

At 20 °C, a marked change in the growth patterns of the *B. cinerea* isolates became apparent. While J5013/3 exhibited a significant increase in growth rate after day 3, the other three strains showed a slower colony expansion. However, since isolates J5021 and J5011/1 exhibited a higher growth rate up until day 4, they had significantly larger colony diameters compared to isolate J5013/3. Isolate J5017 was particularly affected by the temperature increase, displaying the most pronounced reduction in growth. At 25 °C, growth patterns were similar to those observed at 20 °C, with the exception of isolate J5013/3, which exhibited enhanced growth at the higher temperature.

None of the four studied isolates could grow at 30 °C. However, upon transferring plates to 20 °C, the isolates started to grow, with different intensity. Interestingly, J5011/1 and J5017 isolates, which formed the largest and smallest colonies between 20 and 25 °C produced the fastest recovery, while J5013/3 was the least resilient to heat stress (Table 4).

Table 4. Mean colony diameter of isolates incubated at 20 °C, following a heat stress at 30 °C for one week.

Isolate	Colony Diameter (mm, Mean + SE)
J5011/1	71.6 ± 7.88
J5013/3	16.0 ± 16.00
J5017	81.2 ± 6.60
J5021	42.0 ± 17.38

There were no significant differences between the isolates on day 3 of reduced temperature incubation (Kruskal-Wallis test: $p > 0.05$). However, significant differences in colony diameters were observed among the isolates on day 5 (Kruskal-Wallis test: $p < 0.005$) (Figure 7).

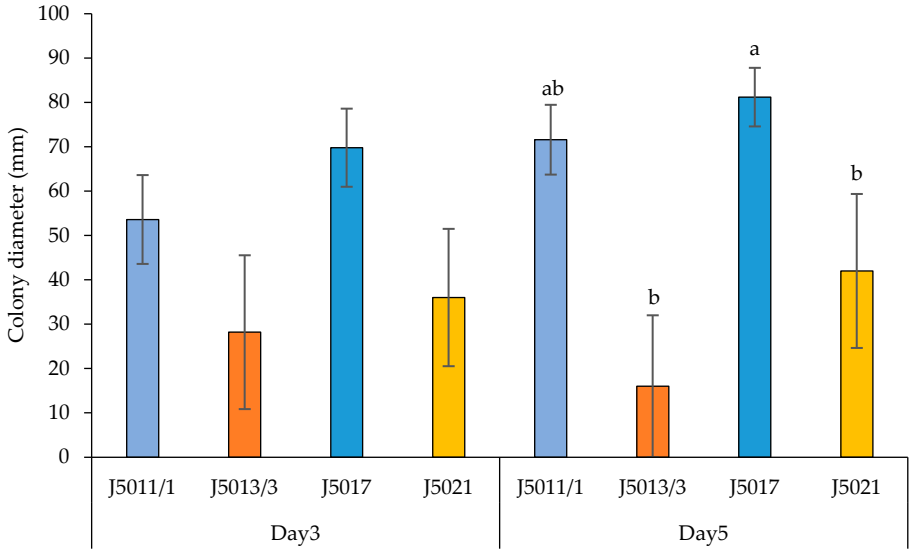

Figure 7. Colony growth of different *Botrytis cinerea* isolates at 20 °C, following a heat stress of 30 °C for one week at 30 °C on the third and fifth days. CLD (lowercase letters) indicates statistical differences based on pairwise Mann-Whitney U tests ($p < 0.05$).

3.5. Pathogenicity Test

Pathogenicity tests conducted at BBCH stage 75 walnut fruits, incubated at 25 °C demonstrated that all *B. cinerea* isolates induced lesions on both the husk and the immature kernel of the walnut. The husk pathogenicity of the four tested fungal pathogens could be categorized into two significantly different groups, based on the severity of the necrotic lesions (Figure 8a). Isolate J5011/1 classified as group b induced significantly more severe lesions with a McKinney index of 60%. However, even this pathogen did not induce complete rot of the husk three weeks after inoculation (Figures 8a and 9b). The wounds on control samples caused only minor damage (Figure 9c). The pathogenicity of the isolates varied when assessed on the kernel (Figure 8b). All four isolates tested differed significantly from the control group. The J5011/1 isolate consistently caused the most severe symptoms, significantly rotting both the husk (Figures 8a and 9a) and the immature kernel (Figures 8b

and 9b). The control samples also exhibited mild symptoms on the kernels, suggesting that physical injury alone can induce some level of damage (Figure 9d).

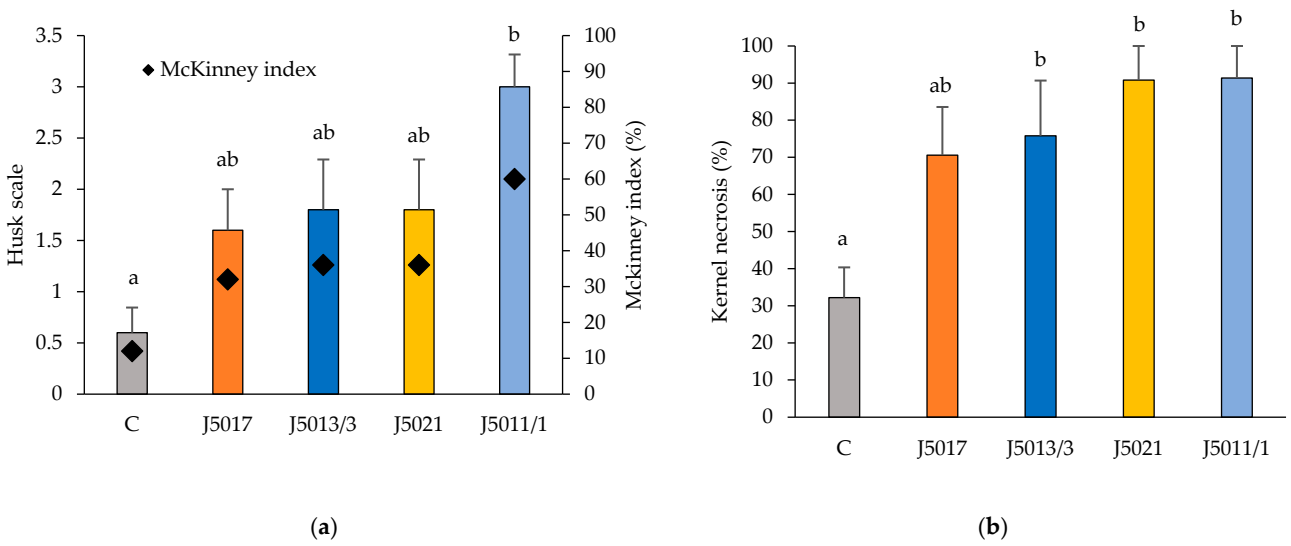

(**a**) (**b**)

Figure 8. (**a**) Scale values and McKinney index on husk and (**b**) percentage of necrosis on walnut kernels at BBCH stage 75 three weeks following inoculation with different *Botrytis cinerea* isolates (J5017, J5013/3, J5021, J5011/1) and a sterile agar plug (C). CLD (lowercase letters) indicates statistically significant differences based on pairwise Mann-Whitney U tests ($p < 0.05$).

Figure 9. Symptoms caused by *Botrytis cinerea* J5011/1 on walnuts BBCH 75 stage three weeks after inoculation. (**a**) Lesions on the surface of the green husks; (**b**) symptoms spreading inside the kernel; symptoms on mocks inoculation (**c**) on the surface of the green husks, (**d**) and around the wound.

Walnut samples at BBCH stage 79, when shell hardening has started, displayed a different response to the pathogen compared to previous trial. The husks showed more severe symptoms (Figure 10a), while the kernels remained unaffected (Figure 10b). While isolates J5021 and J5011/1 caused complete decay of the entire husk in most cases (Figure 10a), isolates J5013/3 and J5017 induced less severe but still significant lesions (Figure 11). Control samples exhibited only minimal browning around the wound (Figure 10c).

Figure 10. Inoculation of walnut at BBCH 79 stage. (**a**) Symptoms on the surface of the husks caused by *Botrytis cinerea* J5021; (**b**) symptoms on kernels inoculated with *B. cinerea* J5021; (**c**) mock inoculation.

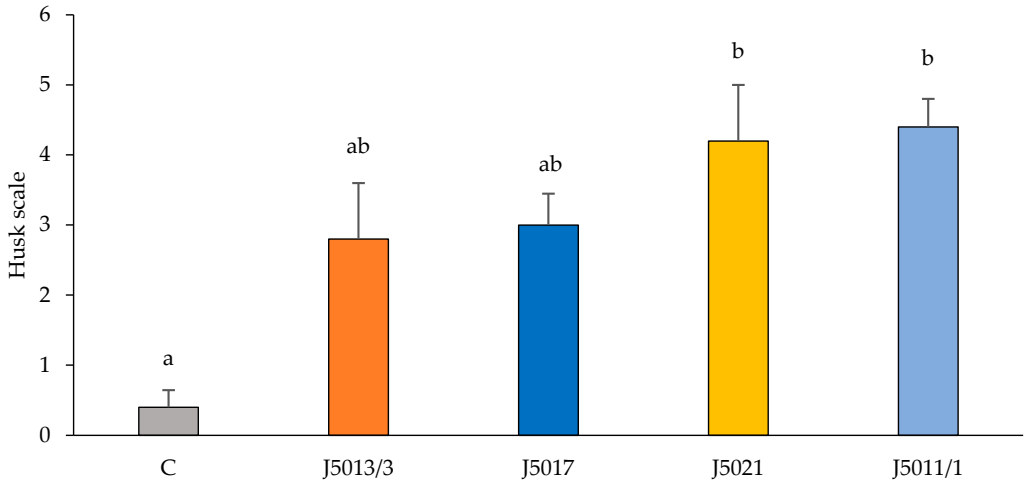

Figure 11. Scale values on mature walnut husk caused by different *Botrytis cinerea* isolates (J5017, J5013/3, J5021, J5011/1), and sterile agar plug (C). CLD (lowercase letters) indicates statistical differences based on pairwise Mann-Whitney U tests ($p < 0.05$).

3.6. Dual Culture of Botrytis cinerea and Trichoderma spp.

Both *Trichoderma* strains inhibited the colony growth of *Botrytis cinerea* isolates as early as three days post-inoculation, with the effect intensifying by the eighth day when the antagonists began overgrowing the pathogen. Strain TR04 showed stronger inhibition than TR05 at this stage (Figures 12 and 13). By the tenth day, both strains had fully overgrown the *B. cinerea* colonies, with TR04 achieving 100% inhibition in all dual cultures, while TR05 reached a maximum inhibition rate of 81% (Figure 12).

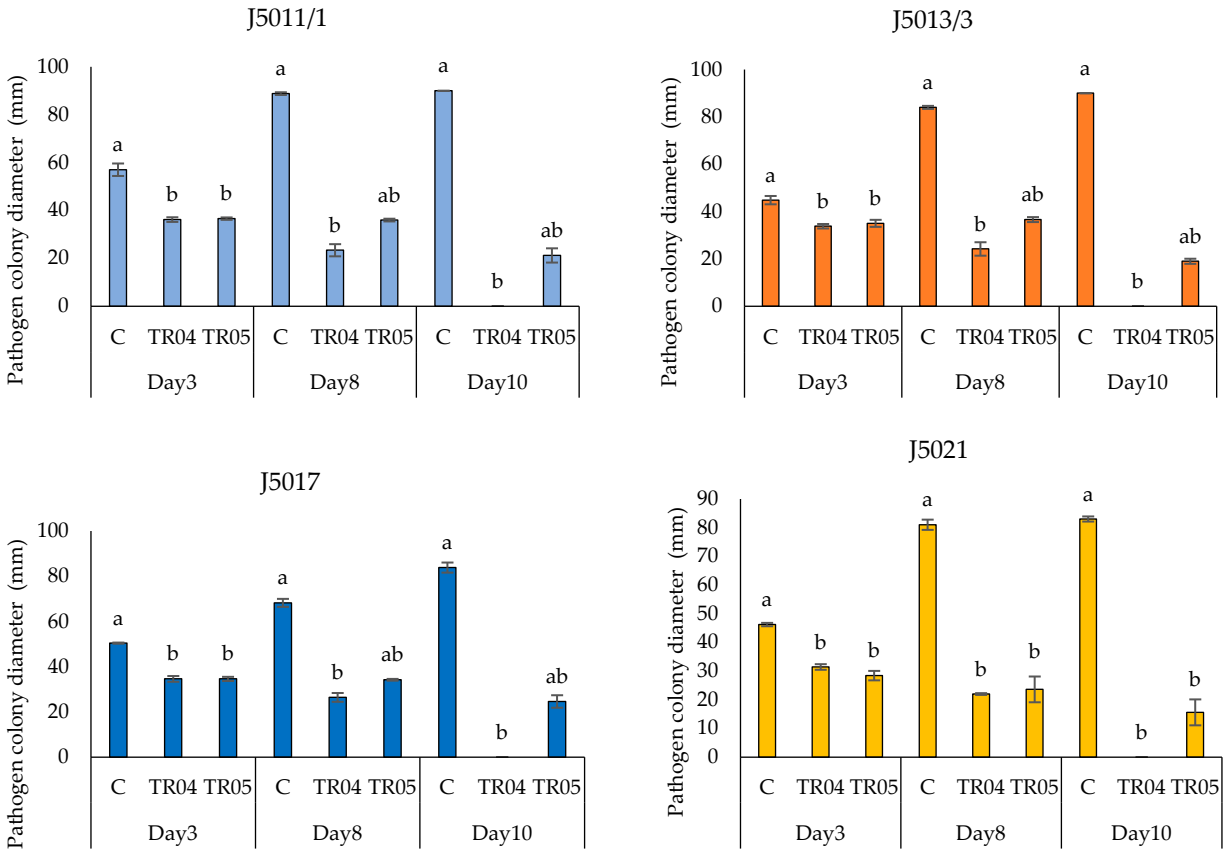

Figure 12. Inhibition of TR04 and TR05 *Trichoderma* strains against *Botrytis cinerea* isolates (J5011/1, J5013/3, J5017, J5021), and without antagonist (C). CLD (lowercase letters) indicates statistical differences based on pairwise Mann-Whitney U tests ($p < 0.05$).

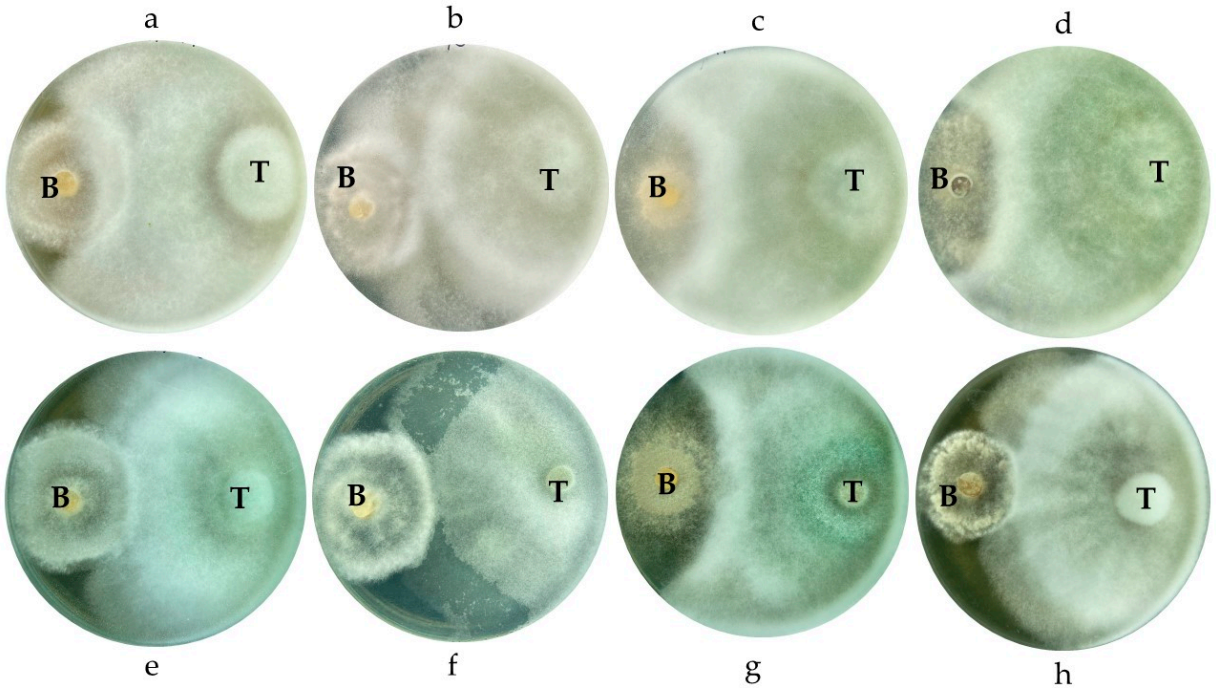

Figure 13. Confrontation test showing the antagonistic activity of *Trichoderma* (T) strains TR04 (**a**–**d**) and TR05 (**e**–**h**) against *Botrytis cinerea* (B) J5011/1 (**a**,**e**), J5013/3 (**b**,**f**), J5017 (**c**,**g**), J5021 (**d**,**h**) eight days after inoculation.

4. Discussion

Walnut cultivation faces increasing challenges, particularly fruit damage and lost. Historically, it was attributed to *Xanthomonas* bacteria [35], however, recent cases of premature walnut drop exhibited distinct symptoms. Green walnuts with brown lesions were collected from a commercial walnut orchard in Hungary, where severe fruit drops and loss was not detected in previous years.

Fungal colonies were not detected during the incubation of the surface sterilized green fruits, therefore the ONFIT method was conducted, which was developed for walnut to identify latent fruit pathogens [25]. We have identified diverse fungal genera on green walnuts, with *Botrytis*, *Aspergillus*, and *Penicillium* being the most prevalent. Previously, *Alternaria*, *Penicillium*, and other fungi (but not *Botrytis*) were detected in symptomatic and asymptomatic walnut kernels in Hungary using ONFIT method [7]. The *Botrytis* genus was dominant with 71% infection rate in green walnuts. Consistent with findings from previous studies [36,37], *B. cinerea* showed highly variable colony morphology. Microscopic characters, like spore size, however are very similar [38]. Thus, molecular identification was carried out to validate the identity of isolates possessing typical microscopic attributes of *B. cinerea*. Based on the sequences of the rDNA region containing ITS1 and 2 regions, the *Botrytis* isolates were identified as *Botrytis cinerea sensu lato* as the causative agent. Previous phylogenetic analysis of 22 *Botrytis* species placed *B. cinerea* in a distinct clade with three related species [39]. While ITS-based analysis offers preliminary identification, definitive species delimitation and confirmation necessitate a polyphasic approach, involving the sequencing and analysis of additional genetic loci, particularly because bootstrap support is commonly weak in *Botrytis* phylogenetic trees [36,40].

Botrytis cinerea, as the second most significant fungal plant pathogen, threatens over 200 crops worldwide [41,42]. This pathogen causes grey mold, impacting flowers, fruits, leaves, shoots, and storage organs such as carrots and sweet potatoes. It significantly affects field crops (e.g., tomato, sunflower, chickpea), vegetables (e.g., broccoli, carrot, cabbage, cucumber, lettuce), and fruits (e.g., strawberries, raspberries, blackberries), particularly in humid greenhouse conditions [42–44]. Additionally, *B. cinerea* is a major postharvest pathogen, damaging stored produce even at near-freezing temperatures [44]. Seedlings in nurseries are also susceptible [45].

Pathogenicity tests and temperature profiling showed that *Botrytis* isolates thrive at 15–25 °C, with optimal growth at 20 °C. At BBCH stages 75 and 79, severe symptoms were observed, though kernel damage was restricted to BBCH 75. The high moisture content and soft texture of immature walnuts at BBCH 75, when shell has not hardened, likely enhance susceptibility, while the hardened shell at BBCH 79 offers partial protection, regardless of severe husk lesions. Despite containing antifungal compounds, *B. cinerea* appears to circumvent host defenses, possibly by modifying metabolic pathways or gene expression [46]. It can also induce ripening, altering chemical composition and defense mechanisms, thereby increasing susceptibility [47]. Infection-related changes in secondary metabolites further reduce antifungal efficacy [48].

B. cinerea thrives at 18–22 °C, but high temperatures (≥32 °C) inhibit mycelial growth and spore germination [49,50]. Notably, none of our isolates grew at 30 °C, but many recovered at 20 °C. Displaying pigmentation and sclerotia formation the isolates indicated potential heat-stress adaptations [50]. These findings, consistent with thermotolerance, suggest certain *B. cinerea* strains might enter a reversible stress state, facilitating their recovery and morphological shifts once optimal conditions are re-established. It is worth noting that brief heat shocks (e.g., 50 °C for 20 s) are reported to trigger plant resistance by activating peroxidase genes and priming defenses without direct fungal inhibition [49,50], but this specific condition was not part of our study. The optimal growth temperature for

Botrytis isolates aligns with Hungary's late spring climate (15–25 °C, particularly from April to June) [51], suggesting high infection potential during walnut flowering (BBCH 60–69) and early fruit development (BBCH 71–79). Pathogenicity tests confirmed that at BBCH 75, *B. cinerea* penetrated and infected kernels, while at BBCH 79, infection was limited to the husk. These findings reinforce that BBCH 75 walnuts are more vulnerable due to their softer texture, higher moisture content, and immature defense system, whereas the hardened shell at BBCH 79 provides partial protection [33]. This was the first detection of *B. cinerea*, with positive patotests on walnut fruits highlighting the need for further study.

With increasing fungicide resistance, limited number of registered fungicide and complicated spraying of the broad and high canopy, finding other sustainable management methods is crucial. *Trichoderma* strains TR04 and TR05 demonstrated significant antagonistic activity, completely overgrowing *Botrytis* isolates in vitro. Their efficacy against *B. cinerea* has been validated in strawberries and tomatoes, supporting their potential as biocontrol agents [52]. *Trichoderma* TR04 and TR05 also exhibited a high in vitro biocontrol index against other walnut pathogens that cause fruit decay (*Botryosphaeria dothidea* and *Diaporthe eres*) [53]. This broad-spectrum activity highlights their promise for comprehensive management of various deteriorating fungal pathogens in walnut orchards.

5. Conclusions

Our study identifies *B. cinerea* as the primary cause of brown spot lesions in immature walnuts, with the pathogen being most aggressive before shell hardening. Its adaptability to optimal growth temperatures and ability to recover post-heat stress may facilitate persistence in walnut orchards. As a sustainable management approach, *Trichoderma* strains TR04 and TR05 show promising potential in controlling *B. cinerea* infections.

Author Contributions: Conceptualization, A.Z., A.C. and E.S.; data curation, A.Z., A.C., L.K. and E.S.; formal analysis, A.Z., A.C. and K.P.; funding acquisition, E.F., L.K. and E.S.; investigation, A.Z., A.C. and K.P.; methodology, A.Z., A.C., K.P. and E.S.; project administration, E.F. and E.S.; resources, E.F., L.K. and E.S.; software, A.C.; supervision, E.S.; validation, K.P., E.F., L.K. and E.S.; visualization, A.Z., A.C. and E.S.; writing—original draft, A.Z., A.C., K.P., E.F., L.K. and E.S.; writing—review and editing, L.K. and E.S. All authors have read and agreed to the published version of the manuscript.

Funding: This research was supported by the Hungarian National Research, Development, and Innovation Fund, grants numbers K 146406 to L.K. and K 138489 to E.F. Supported by the University of Debrecen Program for Scientific Publication.

Data Availability Statement: The raw data supporting the conclusions of this article will be made available by the authors on request.

Acknowledgments: The authors are grateful to Gyula Szakadát for his technical support.

Conflicts of Interest: Erzsébet Sándor receives a royalty for the Trichoderma product containing TR04 *Trichoderma afroharzianum* and TR05 *Trichoderma simmonsii* tested in this study. The rest of the authors declare no conflicts of interest.

Abbreviations

The following abbreviations are used in this manuscript:

ONFIT	Overnight Freezing-Incubation Technique
PDA	Potato Dextrose Agar
ITS	Internal Transcribed Spacer
PCR	Polymerase Chain Reaction
BLAST	Basic Local Alignment Search Tool
NCBI	National Center for Biotechnology Information
MEGA	Molecular Evolutionary Genetics Analysis
BBCH	Biologische Bundesanstalt Bundessortenamt CHemical industry
CLD	Compact Letter Display
rDNA	Rribosomal DNA
SE	Standard Error

References

1. Vahdati, K.; Arab, M.M.; Sarikhani, S.; Sadat-Hosseini, M.; Leslie, C.A.; Brown, P.J. Advances in Persian Walnut (*Juglans regia* L.) Breeding Strategies. In *Advances in Plant Breeding Strategies: Nut and Beverage Crops*; Al-Khayri, J.M., Jain, S.M., Johnson, D.V., Eds.; Springer Nature Switzerland AG: Cham, Switzerland, 2019; Volume 4, pp. 401–472.
2. FAO. Food and Agriculture Organization of the United Nations. Data and Statistics for Walnut. Available online: https://www.fao.org/faostat/en/#data/QCL (accessed on 21 March 2025).
3. Chen, S.F.; Morgan, D.P.; Hasey, J.K.; Anderson, K.; Michailides, T.J. Phylogeny, morphology, distribution, and pathogenicity of Botryosphaeriaceae and Diaporthaceae from English walnut in California. *Plant Dis.* **2014**, *98*, 636–652. [CrossRef] [PubMed]
4. Meng, L.; Yu, C.; Wang, C.; Li, G. First Report of Diaporthe amygdali Causing walnut twig canker in Shandong Province of China. *Plant Dis.* **2018**, *102*, 1859. [CrossRef]
5. Moral, J.; Morgan, D.; Trapero, A.; Michailides, T.J. Ecology and epidemiology of diseases of nut crops and olives diseases caused by Botryosphaeriaceae fungi in California and Spain. *Plant Dis.* **2019**, *103*, 1809–1827. [CrossRef] [PubMed]
6. Zabiák, A.; Kovács, C.; Takács, F.; Pál, K.; Peles, F.; Fekete, E.; Karaffa, L.; Mihály, K.; Flipphi, M.; Sándor, E. *Diaporthe* and *Diplodia* Species Associated with Walnut (*Juglans regia* L.) in Hungarian Orchards. *Horticulturae* **2023**, *9*, 205. [CrossRef]
7. Zabiák, A.; Csótó, A.; Tóth, B.; Takács, F.; Pál, K.; Sándor, E. Identification of *Botryosphaeria dothidea* and *Diaporthe eres* from rotted walnut fruits and other plant parts in different phenological stages. *Acta Phytopathol. Entomol. Hung.* **2023**, *58*, 218–237. [CrossRef]
8. Spence, L.A.; Henschel, B.; Li, R.; Tekwe, C.D.; Thiagarajah, K. Adding Walnuts to the Usual Diet Can Improve Diet Quality in the United States: Diet Modeling Study Based on NHANES 2015–2018. *Nutrients* **2023**, *15*, 258. [CrossRef]
9. Mulrean, E.N.; Schroth, M.N. Ecology of *Xanthomonas campestris* pv. *juglandis* on Persian (English) walnuts. *Phytopathology* **1982**, *72*, 434–438. [CrossRef]
10. Zhang, Q.; Kang, M.; Zhao, R.; Song, L.; Ji, X.; He, A.; Ji, Y. Analysis of the diversity of fungi on green walnut surface based on high-throughput sequencing. *Storage Process* **2024**, *8*, 102–108.
11. Varjas, V.; Lakatos, T.; Tóth, T.; Kovács, C. First report of *Colletotrichum godetiae* causing anthracnose and twig blight on Persian walnut in Hungary. *Plant Dis.* **2020**, *105*, 702. [CrossRef]
12. Li, F.; Chen, J.; Chen, Q.; Liu, Z.; Sun, J.; Yan, Y.; Zhang, H.; Bi, Y. Identification, pathogenicity, and sensitivity to fungicide of *Colletotrichum species* that causes walnut anthracnose in Beijing. *Agronomy* **2023**, *13*, 214. [CrossRef]
13. Zhang, Q.Q.; Shi, J.; Shen, P.Y.; Xi, F.; Qian, C.Y.; Zhang, G.H.; Zhu, H.J.; Xiao, H.M. Exploring the efficacy of biocontrol microbes against the fungal pathogen Botryosphaeria dothidea JNHT01 isolated from fresh walnut fruit. *Foods* **2022**, *11*, 3651. [CrossRef] [PubMed]
14. Çakar, D. Role of the fungal flora on kernel rot of chestnuts. *Uluslararası Tarım Yaban Hayatı Bilim. Derg.* **2023**, *9*, 143–152. [CrossRef]
15. Sun, J.; Zhang, X.; Zheng, J.; Liu, G.; Chen, L. Importance of cell wall permeability and cell wall degrading enzymes during infection of *Botrytis cinerea* in hazelnut. *Forests* **2023**, *14*, 565. [CrossRef]
16. Zheng, X.R.; Huang, X.X.; Peng, J.F.; Gafforov, Y.; Chen, J.J. Occurrence of *Botrytis cinerea* causing gray mold on pecan in China. *Horticulturae* **2024**, *10*, 1212. [CrossRef]
17. Fedele, G.; González-Domínguez, E.; Rossi, V. Influence of Environment on the Biocontrol of *Botrytis cinerea*: A Systematic Literature Review. In *How Research Can Stimulate the Development of Commercial Biological Control Against Plant Diseases, Progress in Biological Control*; De Cal, A., Melgarejo, P., Magan, N., Eds.; Springer: Cham, Switzerland, 2020; Volume 21, pp. 61–82.

18. Hamond, J.B. Ann. Rept. East Malling Rex. Stat. 1928, 1929 and 1930, II Supplement, 1931, pp. 143–149 In: CABI Digital Library. Available online: https://www.cabidigitallibrary.org/doi/full/10.5555/19321100165 (accessed on 21 March 2025).
19. Braithwaite, L.; Braithwaite, M. *Walnut Kernel Mould: Linking Canterbury Research to the Published Scientific Literature*; Plant Diagnostics Limited: Templeton, Christchurch, 2020. Available online: https://walnuts.org.nz/wp-content/uploads/2020/11/Walnut-kernel-decay-review-Final-110920-1.pdf (accessed on 21 March 2025).
20. Fillinger, S.; Elad, Y. *Botrytis—The Fungus, The Pathogen and Its Management in Agricultural Systems*; Springer International Publishing: Cham, Switzerland, 2016.
21. Fernández-Ortuño, D.; Grabke, A.; Li, X.P.; Schnabel, G. Independent emergence of resistance to seven chemical classes of fungicides in *Botrytis cinerea*. *Phytopathology* **2015**, *105*, 424–432. [CrossRef]
22. Druzhinina, I.S.; Chenthamara, K.; Zhang, J.; Atanasova, L.; Yang, D.; Miao, Y.; Rahimi, M.J.; Grujic, M.; Cai, F.; Pourmehdi, S.; et al. Massive lateral transfer of genes encoding plant cell wall-degrading enzymes to the mycoparasitic fungus *Trichoderma* from its plant-associated hosts. *PLoS Genet.* **2018**, *14*, e1007322. [CrossRef]
23. Tyśkiewicz, R.; Nowak, A.; Ozimek, E.; Jaroszuk-Ściseł, J. *Trichoderma*: The current status of its application in agriculture for the biocontrol of fungal phytopathogens and stimulation of plant growth. *Int. J. Mol. Sci.* **2022**, *23*, 2329. [CrossRef]
24. Csótó, A.; Kovács, C.; Pál, K.; Nagy, A.; Peles, F.; Fekete, E.; Karaffa, L.; Kubicek, C.P.; Sándor, E. The biocontrol potential of endophytic *Trichoderma* fungi isolated from Hungarian grapevines, Part II, Grapevine stimulation. *Pathogens* **2023**, *12*, 2. [CrossRef]
25. Michailides, T.J.; Morgan, D.P.; Felts, D. Detection and significance of symptomless latent infection of *Monilinia fructicola* in California stone fruits. *Phytopathology* **2000**, *90*, S53.
26. Michailides, T.J.; Morgan, D.P.; Luo, Y. Epidemiological Assessments and Postharvest Disease Incidence. In *Postharvest Pathology. Plant Pathology in the 21st Century (Contributions to the 9th International Congress)*; Prusky, D., Gullino, M., Eds.; Springer: Dordrecht, The Netherlands, 2009; Volume 2. [CrossRef]
27. Kovács, C.; Peles, F.; Bihari, Z.; Sándor, E. Endophytic fungi associated with Grapevine Trunk Diseases, from Tokaj wine region, Hungary. *Növényvédelem* **2014**, *50*, 153–159.
28. Pezet, R.; Viret, O.; Perret, C.; Tabacchi, R. Latency of *Botrytis cinerea* Pers.: Fr. and biochemical studies during growth and ripening of two grape berry cultivars, respectively susceptible and resistant to grey mould. *J. Phytopathol.* **2003**, *151*, 208–214. [CrossRef]
29. Thi Minh Le, T.; Thi Hong Hoang, A.; Thi Bich Le, T.; Thi Bich Vo, T.; Van Quyen, D.; Hoang Chu, H. Isolation of endophytic fungi and screening of Huperzine A–producing fungus from *Huperzia serrata* in Vietnam. *Sci. Rep.* **2019**, *9*, 16152. [CrossRef] [PubMed]
30. White, T.J.; Bruns, T.; Lee, S.; Taylor, J.W. *PCR Protocols: A Guide to Methods and Applications*; Academic Press: New York, NY, USA, 1990; p. 482.
31. Kumar, S.; Stecher, G.; Tamura, K. MEGA7: Molecular Evolutionary Genetics Analysis version 7.0 for bigger datasets. *Mol. Biol. Evol.* **2016**, *33*, 1870–1874. [CrossRef]
32. Kimura, M. A simple method for estimating evolutionary rate of base substitutions through comparative studies of nucleotide sequences. *J. Mol. Evol.* **1980**, *16*, 111–120. [CrossRef]
33. Robin, J.; Bernard, A.; Albouy, L.; Papillon, S.; Tranchand, E.; Hebrard, M.N.; Philibert, J.B.; Barbedette, M.; Schafleitner, S.; Wenden, B.; et al. Description of Phenological Events of Persian Walnut (*Juglans regia* L.) according to the Extended BBCH Scale and Historical Scales. *Horticulturae* **2024**, *10*, 402. [CrossRef]
34. McKinney, H.H. Influence of soil temperature and moisture on infection of wheat seedlings by *Helmintosporium sativum*. *J. Agric. Res.* **1923**, *26*, 195–218.
35. Lamichhane, J.R. *Xanthomonas arboricola* Diseases of Stone Fruit, Almond, and Walnut Trees: Progress Toward Understanding and Management. *Plant Dis.* **2014**, *98*, 1600–1610. [CrossRef]
36. Garfinkel, A.R.; Coats, K.P.; Sherry, D.L.; Chastagner, G.A. Genetic Analysis Reveals Unprecedented Diversity of a Globally-Important Plant Pathogenic Genus. *Sci. Rep.* **2019**, *9*, 6671. [CrossRef]
37. Dučkena, L.; Bimšteine, G.; Bankina, B.; Skinderskis, E.; Roga, A.; Frīdmanis, D. Morphological diversity and mycelial compatibility of *Botrytis pseudocinerea* and *Botrytis cinerea* isolated in Latvia. *Proc. Latv. Acad. Sci.* **2024**, *78*, 197–205. [CrossRef]
38. Fekete, É.; Fekete, E.; Irinyi, L.; Karaffa, L.; Árnyasi, M.; Asadollahi, M.; Sándor, E. Genetic diversity of a *Botrytis cinerea* cryptic species complex in Hungary. *Microbiol. Res.* **2012**, *167*, 283–291. [CrossRef]
39. Staats, M.; van Baarlen, P.; van Kan, J.A.L. Molecular phylogeny of the plant pathogenic genus *Botrytis* and the evolution of host specificity. *Mol. Biol. Evol.* **2005**, *22*, 333–346. [CrossRef] [PubMed]
40. Lukasko, N.T.; Hausbeck, M.K. Whole-genome resource of seven *Botrytis cinerea sensu lato* isolates with resistance or sensitivity to seven site-specific fungicides. *Phyto Front.* **2024**, *4*, 251–254. [CrossRef]
41. Dean, R.; Van Kan, J.A.; Pretorius, Z.A.; Hammond-Kosack, K.E.; Di Pietro, A.; Spanu, P.D.; Rudd, J.J.; Dickman, M.; Kahmann, R.; Ellis, J.; et al. The Top 10 fungal pathogens in molecular plant pathology. *Mol. Plant Pathol.* **2012**, *13*, 414–430. [CrossRef] [PubMed]

42. Elad, Y.; Pertot, I.; Cotes Prado, A.M.; Stewart, A. Plant Hosts of *Botrytis* spp. In *Botrytis—The Fungus, the Pathogen and Its Management in Agricultural Systems*; Fillinger, S., Elad, Y., Eds.; Springer: Cham, Switzerland, 2016; pp. 1–15. [CrossRef]
43. Pande, S.; Galloway, J.; Gaur, P.M.; Siddique, K.H.M.; Tripathi, H.S.; Taylor, P.; MacLeod, M.W.J.; Basandrai, A.K.; Bakr, A.; Joshi, S.; et al. Botrytis grey mould of chickpea: A review of biology, epidemiology, and disease management. *Aust. J. Agric. Res.* **2006**, *57*, 1137–1150. [CrossRef]
44. Droby, S.; Lichter, A. Post-Harvest Botrytis Infection: Etiology, Development and Management. In *Botrytis: Biology, Pathology and Control*; Elad, Y., Williamson, B., Tudzynski, P., Delen, N., Eds.; Springer: Dordrecht, The Netherlands, 2007; pp. 349–367. [CrossRef]
45. Williamson, B.; Tudzynski, B.; Tudzynski, P.; van Kan, J.A.L. *Botrytis cinerea*: The cause of grey mould disease. *Mol. Plant Pathol.* **2007**, *8*, 561–580. [CrossRef]
46. Kuroyanagi, T.; Bulasag, A.S.; Fukushima, K.; Ashida, A.; Suzuki, T.; Tanaka, A.; Camagna, M.; Sato, I.; Chiba, S.; Ojika, M.; et al. *Botrytis cinerea* identifies host plants via the recognition of antifungal capsidiol to induce expression of a specific detoxification gene. *PNAS Nexus* **2022**, *1*, pgac274. [CrossRef]
47. Silva, C.J.; Adaskaveg, J.A.; Mesquida-Pesci, S.D.; Ortega-Salazar, I.B.; Pattathil, S.; Zhang, L.; Hahn, M.G.; van Kan, J.A.L.; Cantu, D.; Powell, A.L.T.; et al. *Botrytis cinerea* infection accelerates ripening and cell wall disassembly to promote disease in tomato fruit. *Plant Physiol.* **2023**, *191*, 575–590. [CrossRef]
48. Wu, Z.; Gao, T.; Liang, Z.; Hao, J.; Liu, P.; Liu, X. Dynamic changes in plant secondary metabolites induced by *Botrytis cinerea* infection. *Metabolites* **2023**, *13*, 654. [CrossRef]
49. Widiastuti, A.; Yoshino, M.; Saito, H.; Maejima, K.; Zhou, S.; Odani, H.; Hasegawa, M.; Nitta, Y.; Sato, T. Induction of disease resistance against *Botrytis cinerea* by heat shock treatment in melon (*Cucumis melo* L.). *Physiol. Mol. Plant Pathol.* **2011**, *75*, 157–162. [CrossRef]
50. Zhang, M.; Trushina, N.K.; Lang, T.; Hahn, M.; Pasmanik-Chor, M.; Sharon, A. Serine peptidases and increased amounts of soluble proteins contribute to heat priming of the plant pathogenic fungus *Botrytis cinerea*. *mBio* **2023**, *14*, e0107723. [CrossRef]
51. Hungarian Meteorological Service. Temperature in Hungary. HungaroMet. Available online: https://www.met.hu/en/eghajlat/magyarorszag_eghajlata/altalanos_eghajlati_jellemzes/homerseklet/ (accessed on 12 October 2024).
52. Geng, L.; Fu, Y.; Peng, X.; Yang, Z.; Zhang, M.; Song, Z.; Guo, N.; Chen, S.; Chen, J.; Bai, B.; et al. Biocontrol potential of *Trichoderma harzianum* against *Botrytis cinerea* in tomato plants. *Biol. Control* **2022**, *174*, 105019. [CrossRef]
53. Kovács, C.; Csótó, A.; Pál, K.; Nagy, A.; Fekete, E.; Karaffa, L.; Kubicek, C.P.; Sándor, E. The biocontrol potential of endophytic *Trichoderma* fungi isolated from Hungarian grapevines. Part I. Isolation, identification and in vitro studies. *Pathogens* **2021**, *10*, 1612. [CrossRef]